A New Technique for Detailed Acoustic Current Profiles in the Continental Shelf Wave Bottom Boundary Layer

Archie T. Morrison III

Department of Applied Ocean Physics and Engineering
Woods Hole Oceanographic Institution
Woods Hole, Massachusetts 02543

Abstract - **High bottom stress levels in the continental shelf wave bottom boundary layer make it of great importance in the study of sediment entrainment and transport. Existing instruments capable of making measurements in the wave boundary layer cannot resolve its full dynamic behavior because they are restricted to single measurement volumes. An acoustic current meter with multiple sample volumes in a geometry designed to resolve the primary scales of flow in the wave bottom boundary layer is described. The capabilities of the proposed instrument are compared to those of existing techniques and a preliminary error analysis is performed.**

I. INTRODUCTION

The continental shelf wave bottom boundary layer is a thin sheet of oscillatory shear flow generated by surface swell. The thinness of the layer is responsible for bottom shear stresses which may be up to an order of magnitude greater than the bottom stresses associated with a mean flow of comparable magnitude. The wave induced bottom shear is capable of initiating sediment motion in relatively mild sea states. The wave boundary layer thus plays a central role in the entrainment of sediment into the water column. The high stress levels also increase the turbulent dissipation of flow energy. As a result, the mean flow experiences an apparent bottom roughness much larger than the scale of the physical roughness elements [7, 8, 9, 13].

Investigations into the structure of the wave boundary layer in the laboratory and through analytical and semi-empirical models have primarily focused on monochromatic, unidirectional waves over relatively simple, non-erodable bottom geometries. A concise summary listing of much of this work can be found in Trowbridge and Agrawal [16]. Of particular note are the measurements made by Jonsson and Carlsen [11]. Additionally, a complete, semi-empirical model with considerable complexity and range has been described by Madsen [13].

Conditions on the shelf are significantly more complicated than those that can commonly be created in the laboratory or in a model, however. The wave field is neither monochromatic nor unidirectional in general and the sediment is highly variable spatially and temporally over a range of characteristics. Conley and Inman [6] report, for example, an asymmetry in bed response between wave crest and wave trough observed in the field which is not reproduced in laboratory experiments which otherwise achieve hydrodynamic similitude. Greater understanding of the wave boundary layer requires high quality measurements made on the continental shelf.

Relatively high resolution field measurements have been made using heated thermistors [4, 5], hot wires and films [6, 10], and laser doppler velocimeters (LDVs) [1, 2, 16]. These are important and interesting results, but they do not resolve the dynamic structure of the wave boundary layer. The limitation inherent in these instruments is their dependence on a single measurement volume which must be mechanically scanned through the boundary layer to obtain a profile. The scan rate is limited by flow disturbance considerations and by the noise level of individual measurements. All of these devices require averages over many samples to achieve good velocity resolution. The high sampling rates possible with these instruments allow observation of turbulent spectra, but vertical correlations through the boundary layer are not available and profiles are necessarily ensemble averages over several wave cycles.

Additionally, these techniques have some limitations with respect to resolution and robustness under field conditions. Hot wires can resolve a few tenths of a millimeter per second, but they are physically quite fragile. They are very sensitive to fouling which causes drift of the nonlinear response. Calibration can be lost in less than a minute. Hot films are mechanically tougher, but less sensitive (millimeter per second resolution) and suffer the same rapid fouling problems. Heated thermistors have better mechanical toughness, but are otherwise comparable to hot films. All three devices give speed but not directional information. LDVs depend on particle concentrations in a range that keeps the sample volume occupied without attenuating the beam below the detection limit. Velocity resolution is several millimeters per second and the output includes both magnitude and direction. These limitations are not insurmountable and these instruments, although they are primarily laboratory techniques, have been adapted for field use.

This paper provides an overview of the ongoing development of an instrument designed to resolve in detail the dynamic velocity structure of the continental shelf wave bottom boundary layer. The design addresses the instrument limitations discussed above, most notably by using multiple measurement volumes. Necessarily there are design trade-offs and the limitations inherent in the proposed instrument will also be discussed. The scales of flow in the wave bottom boundary layer are determined in Section II. This information is used in the design of the instrument in Section III. A preliminary error analysis is made in Section IV and a brief assessment of the instrument's capabilities is made in Section V.

This work is being supported by AASERT funding under ONR contract N00014-89-J-1058. WHOI Contribution No. 8864.

0-7803-2437-4/95/$4.00.

II. CHARACTERISTIC SCALES

Resolving the dynamic structure of the wave bottom boundary layer, as with any process, requires accurate measurements with spatial and temporal spacings that are small compared with the characteristic scales of flow in the layer. The fundamental time scale is the wave period, T. Surface swell with periods from 5 s to 20 s is ubiquitous on the continental shelf. Sample rates of several Hertz will be adequate for the wave motion.

The fundamental vertical length scale is the thickness of the wave bottom boundary layer. Following Grant and Madsen [8] and assuming a turbulent flow, the thickness, δ_w, is scaled by the shear velocity and the wave frequency.

$$\delta_w = \frac{\kappa u_{*m}}{\omega} \tag{1}$$

where $\kappa = 0.4$ is von Karman's constant, $u_{*m} = \sqrt{\tau_m/\rho}$ is the maximum shear velocity, τ_m is the maximum bottom shear stress, ρ is the density of sea water, and ω is the radian frequency of the wave. On the shelf, δ_w is on the order of a centimeter, typically falling between 5 mm and 20 mm. Alternatively, an assumption of laminar flow in the wave boundary layer would scale the thickness with the kinematic viscosity, ν, and the wave frequency [12].

$$\delta_w = 4\sqrt{\frac{\nu}{\omega}} \tag{2}$$

The laminar thickness falls in a range from 4 mm to 8 mm on the shelf. In both cases there are variations of the boundary layer velocity about u_b, the velocity outside the wave boundary layer, above δ_w. However, these variations are small compared to the variations below δ_w.

Conley and Inman [6] have argued that under near breaking waves at the edge of the surf zone, the wave bottom boundary layer can alternate between laminar and turbulent flow inside a transitional range of the wave Reynolds number, $RE = u_{bm}^2/\omega\nu$, where u_{bm} is the maximum orbital velocity at the bottom. Below or above that range the layer is purely laminar or purely turbulent. Grant and Madsen [8] and Trowbridge and Agrawal [16] expect that the wave boundary layer on the shelf will generally be turbulent. Jonsson and Carlsen [11] maintain that oscillatory flow near the bed under waves in the coastal zone is always rough turbulent. The model in the recent work by Madsen [13] employs both smooth and rough turbulent regimes which are a reasonable match to the observations of Conley and Inman [6]. Given the variability of bottom conditions on the shelf, it is not unreasonable to expect both laminar and turbulent wave boundary layers. Vertical spacing of sampling volumes at millimeter or finer intervals is necessary in either case.

On a flat bed there are two horizontal length scales of interest, the wave length and the orbital excursion amplitude. The wave length, λ, scales the distance over which wave velocities change. Wave lengths on the shelf are typically tens to hundreds of meters. This does not seriously constrain the horizontal extent of the sample volume. The orbital excursion amplitude at the bottom, A_{bm}, can be calculated from linear wave theory.

$$A_{bm} = \frac{u_{bm}}{\omega} = \frac{a\omega}{\sinh(kh)}\frac{1}{\omega} \tag{3}$$

where k is the wave number, and h is the water depth. On the shelf the excursion amplitude can range up to one or two meters. Values from 10 cm to 50 cm are typical. The field of turbulent fluctuations advected through the sample volume is determined by A_{bm}. Therefore the horizontal extent of the sample volume should be kept small compared to the excursion amplitude.

Bedforms create additional length scales. For the case of wave generated ripples in equilibrium with the flow, Wiberg and Harris [17] have shown that the bedform scales are determined by the ratio A_{bm}/d_g, where d_g is the grain diameter. For $A_{bm}/d_g < \approx 10^3$, the ripple wave length, λ_b, and the ripple height, η_b, are scaled by A_{bm}. Under these conditions, which are common in the laboratory, $\eta_b > \delta_w$ and a well defined wave boundary layer does not form. On the shelf the ratio is normally larger than 10^3 and the ripples are scaled by d_g. $\lambda_b \approx 10$ cm is a representative value. Typically $\eta_b < \delta_w$ so that a well defined wave boundary layer can form [17]. These results indicate that ripple geometry can be a more severe constraint on sample volume size than the excursion amplitude. Less organized bedforms present additional difficulties. Making measurements among bedforms is difficult and requires resolution of both horizontal and vertical velocities.

Other phenomena of interest include turbulence, bursting and sweeping, streaming, and the viscous sublayer. Following Kundu [12], the largest turbulent eddies scale with the boundary layer thickness and turbulent fluctuations scale with the shear velocity. The dissipation rate, ε, then scales as

$$\varepsilon \sim \frac{u'^3}{l} \sim \frac{u_{*m}^3}{\delta_w} \tag{4}$$

For typical shelf values the dissipation rate is of order 1 cm^2/s^3. Kolmogorov's microscale for viscous dissipation is

$$\eta = \left(\frac{\nu^3}{\varepsilon}\right)^{1/4} \tag{5}$$

For the dissipation rate given above, the viscous microscale is a few tenths of a millimeter. Measurement intervals should be smaller than $\eta/2$ to resolve the full extent of the inertial and dissipating subranges of the turbulent spectrum. This requires a brief digression.

The desirability of multiple sensing volumes was established in Section I. The circuit complexity associated with submillimeter spacing over several centimeters makes vertical spacing finer than millimeter scale doubtful in this situation. In the presence of a net advective flow, however, finer measurement intervals can be achieved temporally as the field of turbulent fluctuations, assumed frozen, is advected past the sensor. This approach will work for the horizontal flow in the wave boundary layer. Therefore, while the turbulent spectrum for $k_v\eta \rightarrow 1$, where k_v is the vertical turbulent wave number, may not be directly accessible, the spectrum for $k_h\eta \rightarrow 1$, where k_h is the horizontal turbulent wave number, should be. Turbulence in a shear layer is expected to be anisotropic only for values of $k\eta \ll 1$ (i.e., for $kz = O(1)$, where z is height above the bottom). Both spectra are therefore recoverable down to the dissipation subrange, provided the noise level in the velocity measurement is sufficiently low and the measurement volume is sufficiently small. If the microscale depends only

on ε and ν, then dimensional analysis suggests a time scale

$$t_\eta \sim \left(\frac{\nu}{\varepsilon}\right)^{1/2} \tag{6}$$

which is of order 10^{-1} s and thus a velocity scale

$$u_\eta = \eta/t_\eta = (\nu\varepsilon)^{1/4} \tag{7}$$

which is of order 1 mm/s. Velocity resolution of order 10^{-1} mm/s is indicated. Note that this would also be sufficient for the primary flow where discrimination of velocity differences down to order 1 mm/s may be required. However, the measurement volume is not easily reduced to the the scale of η. The visible portion of the inertial subrange will be limited by the dimensions of the measurement volume.

Bursting and sweeping are turbulent boundary layer phenomena. A discussion can be found in Kundu [12]. Briefly, vortices oriented parallel to the boundary and perpendicular to the flow are distorted and stretched away from (bursting) or towards (sweeping) the boundary. The phenomena are quasi-periodic and increase the vertical exchange of horizontal momentum. The sweeping of higher speed water closer to the boundary has been observationally linked with the initiation of sediment motion in a wave boundary layer [6]. Semi-empirical relationships predicting the period and the cross-stream and streamwise spacing are given by Conley and Inman [6].

$$\frac{T_s u_{bm}}{\delta_w} \approx 5 \tag{8}$$

$$s^+ \sim \frac{s u_{*m}}{\nu} \approx 100 \tag{9}$$

$$l_s = T_s u_{bm} = 5\delta_w \tag{10}$$

where T_s is the period, s^+ and s are the dimensionless and dimensional cross stream spacing, and l_s is the streamwise spacing. These expressions were originally derived for unidirectional, turbulent flow, but they are in reasonable agreement with wave boundary layer observations made in near breaking waves [6]. For shelf conditions, assuming these relationships are valid, bursting and sweeping occur at a frequency of approximately 3 Hz with spacing of 1 cm cross-stream and 5 cm along stream. Sampling rates near 10 Hz and sampling volumes smaller than 1 cm^3 are indicated.

Streaming is a second order steady flow that occurs in oscillatory boundary layers where asymmetries exist. The horizontal variation of the horizontal velocity causes a small vertical velocity because of continuity. If the two velocities are not precisely in quadrature, due to dissipation for example, net vertical transfer of horizontal momentum occurs. The result is a steady horizontal flow. Batchelor [3] suggests that the streaming velocity, u_s, is scaled by the irrotational oscillation velocity, the wave frequency, and the wave length.

$$u_s \sim \frac{u_b^2}{\omega\lambda} \tag{11}$$

Equivalently, recall that streaming is a function of the convective acceleration terms in the equations of motion. Those terms are of order u/c compared to the retained terms in the linearized boundary layer equations. On the shelf u_s is of order 10^0 mm/s to 10^{-1} mm/s with the larger portion of the range more common in shallow depths. These velocities are up to an order of magnitude below the velocities of the turbulent microscale and will be difficult or impossible to detect.

When the boundary is sufficiently smooth, a viscous sublayer forms beneath the logarithmic layer of a boundary layer flow. Caldwell and Chriss [4, 5] made measurements at 200 m in a steady tidal flow with a heated thermistor strongly suggesting the existence of a viscous sublayer in the ocean. They recorded a sublayer thickness of 5 mm to 10 mm with velocities up to 6 cm/s. An instrument capable of resolving the wave bottom boundary layer will also be able to resolve a steady viscous sublayer. However, the thickness of the viscous sublayer scales with the kinematic viscosity and the shear velocity [12].

$$\delta_v \simeq \frac{5\nu}{u_{*m}} \tag{12}$$

The viscous sublayer thickness beneath the wave bottom boundary layer on the shelf will be less than a millimeter. As previously discussed, it is doubtful that spatial resolution below millimeter scales can be achieved.

III. INSTRUMENT DESIGN

The proposed instrument will be based on the BASS [18] differential travel time technique using ceramic piezoelectric transducers in a geometry tailored to investigation of the wave bottom boundary layer. Figure 1 is a schematic representation of the basic sensor geometry. Because of its appearance the instrument is referred to as the "BASS Rake". The transducers are mounted in 4 slender vertical tines arranged in a square. Two intersecting acoustic paths at each measurement level will determine the horizontal velocity vector. There are 36 measurement levels with 1 mm vertical spacing between 0 mm and 35 mm above the bottom. Figure 2 shows this portion of the array in detail. There are 10 additional measurement levels with logarithmic spacing between 4 cm and 30 cm above the bottom. Above that level a standard BASS tripod is a more suitable instrument.

The transducer pattern was chosen to maximize the number of measurements made in the wave boundary layer. Above that level velocity changes more slowly with height and coarser vertical sampling is appropriate. The logarithmic spacing simply reflects the structure of the boundary layer. The flow is expected to be strongly horizontal within 30 cm of the bottom. Vertical measurements can be made flexibly as circumstances dictate, but the emphasis of the design is on measurement of horizontal motion.

The transducers are piezoelectric disks 2.5 mm in diameter and 1.1 mm thick. The view along a tine of a single mounting within the dense array is shown in Figure 3. The transmitting face is mounted on a flat strip of aluminum to which it is also electrically connected along the edge of the disk using silver epoxy. Signal connections are made through fine transformer wire attached to the back face of the transducer. A halfround aluminum channel covers the connections. The aluminum strip and channel provide mechanical stiffness, a signal return path, and a shield against capacitive coupling with the sea water.

The volume enclosed by the channel and strip is filled with EN-2 polyurethane. EN-2 was developed for use

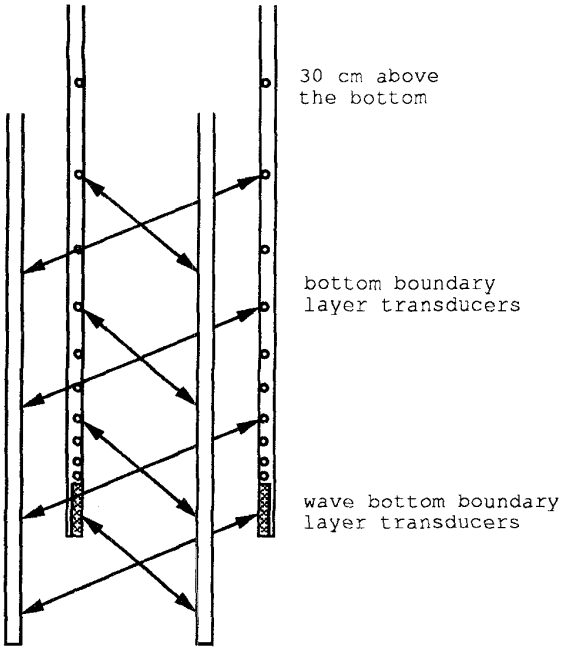

Figure 1. BASS RAKE ACOUSTIC TRANSDUCER GEOMETRY - Transducers are mounted in a high density array in the bottom 3.5 *cm* of each tine. Additional transducers are mounted with logarithmic spacing between 4 *cm* and 30 *cm* above the bottom. The tines are 8 *mm* in diameter. Crossing horizontal acoustic paths measure the horizontal velocity vector. The instrument should be oriented with approximately a 45° angle between the acoustic paths and the prevailing flow to reduce wake effects along the acoustic path.

with transformer windings and has a very low viscosity before setting. The low viscosity makes it relatively easy, during the curing process, to remove air bubbles trapped among the signal wires during injection of the urethane. EN-2 is also used on the mounting shoulder to provide some compliance in the mount. The cylindrical tine is then filled out and sealed using EN-4 polyurethane. EN-4 is less forgiving than EN-2 and considerable care must be taken during the potting process. However, EN-4 has well described acoustic properties which recommend its use here. Most importantly, the acoustic refraction index of this polyurethane very closely matches the acoustic refraction index of water. The asymmetric covering over the transducer will not deflect the acoustic beam.

The choice of this transducer geometry was largely driven by the structures of the wave bottom boundary layer and the flow immediately above it. However, the four tines, particularly the capacitive coupling shield and the transformer wires immbedded in urethane, also make accurate calibration of the BASS Rake straightforward. Capacitive variations in the transducers and the harness leading to the receivers produce offsets in the output. For example, the coaxial cables used on a BASS tripod are responsible for flexure and pressure dependent offsets in the measured velocity. Constant offsets can be accurately removed during calibration with carrageenan gel [14]. The channel and aluminum strip shield the signal wires from variable coupling with the seawater, but they do not form a pressure seal. Pressure is transferred by the urethane

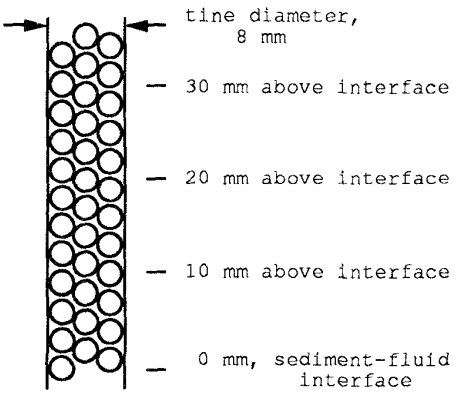

Figure 2. TRANSDUCER ARRAY FOR THE WAVE BOTTOM BOUNDARY LAYER - A dense transducer array is used along the bottom 35 *mm* of the sensor to resolve the behavior of the wave bottom boundary layer. The transducers are 2.5 *mm* in diameter and operate at a frequency of 1.75 MHz. The ratio of beam width at the receiver to path length is approximately 0.9 providing a wide main lobe. Vertical velocities are measured by selecting a receiver within the main lobe but at a different height from the transmitting transducer. All transducers can be used for both horizontal and vertical velocity measurements.

so that all sides of the transducers, strip, and channel are exposed to the same pressure. Thus there is no deflection of the shield with depth as there is with coaxial cable. The urethane also prevents flexure of the wires, removing another variable effect present with coax. Finally, carrageenan gel can be easily molded to fill the acoustic volume for determination of the zero flow offsets.

Using the differential travel time technique the velocity along an acoustic axis is calculated from

$$u_{axis} = \frac{c^2 \Delta t}{2l} \tag{13}$$

where c is the speed of sound, Δt is the difference in travel time, and l is path length. The single measurement differential time resolution is 40 *ps*. This is achieved by making both forward and reversed measurements to remove any bias in the receivers. For a 15 *cm* path length the velocity accuracy is 0.3 mm/s over a linear dynamic range of ± 240 cm/s. The duration of the measurement cycle for a single path is aproximately 320 μs of which 220 μs is acoustic travel time (once again assuming a 15 *cm* path length). All 92 acoustic axes of the BASS Rake can be sampled within a 30 *ms* window. There is some additional overhead associated with calculation and storage, but a 10 Hz sampling rate presents no difficulties. Sampling at up to 33 Hz is possible for periods of time limited by the availability of RAM [18, 14].

The 2.5 *mm* diameter of the transducers is the smallest that can be easily manufactured. A larger diameter would make millimeter vertical spacing difficult. The 1.75 MHz pulse has a beam width to path length ratio of 0.9. This is a very wide main lobe and may cause a second arrival depending on bottom characteristics and path height. This will be explored with a planned prototype. The beam width could be reduced by using a higher frequency. However, this would require a signif-

icant redesign of existing circuitry and will be avoided if possible. One benefit of the wide beam will be the ability to make vertical velocity measurements from any transducer.

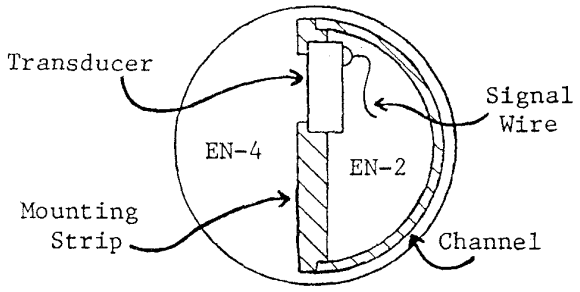

Figure 3. TRANSDUCER MOUNT - The view is a section across a tine assembly at the level of a transducer in the dense portion of the array.

IV. ERROR ANALYSIS

The tines represent a flow obstruction which can completely compromise a measurement when the flow is parallel to one of the acoustic paths. For this reason the instrument must be deployed such that the prevailing velocity forms approximately a 45° angle with both acoustic paths. This presents no difficulty in a laboratory setting. On the shelf, where prevailing motions commonly change direction, this may be achieved by deploying multiple BASS Rakes with different orientations from a central structure. The output of a BASS current meter could be used to select uncompromised data from the multiple records.

Even with proper orientation, the tines create a flow disturbance comprised of potential flow distortions and wake effects. The induced errors depend on flow speed, u, tine diameter, $D = 8\ mm$, and path length, l. The error due to potential flow distortion by a single tine, Δu_{PF}, can be obtained by integrating the velocity distortion [12] along the acoustic path.

$$\frac{\Delta u_{PF}}{u} = \frac{D^2}{4l}\left[\frac{1}{l} - \frac{1}{D/2}\right]\cos\theta \approx 0.7\frac{D}{l} \qquad (14)$$

Because of symmetry, the contributions of the four tines cancel in the center. However, there is also constructive interference of the potential fields due to the implicit integration along the acoustic path. To be conservative, the four tines are treated as independent contributors to the total error in the calculation below.

Following Trivett, Terray, and Williams [15], wake induced errors can be attributed to the velocity defect and vortex shedding.

$$\frac{\Delta u_{VD}}{u} = 0.66 C_D \frac{D}{l} \qquad (15)$$

$$\frac{\Delta u_{VS}}{u} = 0.02\frac{D}{l} \qquad (16)$$

where Δu_{VD} is the velocity defect error and Δu_{VS} is the velocity error caused by vortex shedding. The latter is small due to path averaging. C_D, the drag coefficient, is approximately 1 given the Reynolds and Keulegan-Carpenter numbers of the flow. The constant in Equation 16 is scaled up from that given in [15] assuming a linear relationship in D/l. The original constant was empirically derived from spectral data for a particular strut diameter and path length. All of these formulas are based on simplifying assumptions and should not be depended on for precise quantitative information. In particular, Equation 15 is a far field wake solution being applied in the near field. Arguably, because of the geometry of the BASS Rake, these formulas overpredict the error for uniform flow. However, the oscillatory nature of the flow being investigated causes complicated wake interactions with an effect on the error that is diffucult to quantify. A conservative design and empirical testing are indicated.

An error surface plotted as a function of velocity and path length is shown in Figure 4. The error is calculated from Equations 14, 15, and 16 assuming the errors are independent. Fairing the tines may be a suitable way

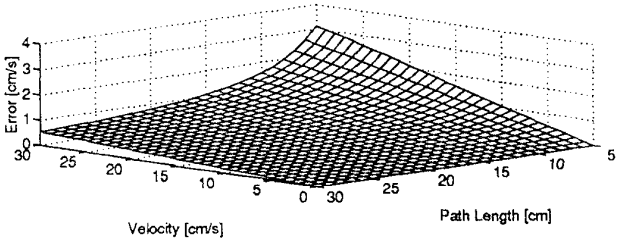

Figure 4. BASS RAKE ERROR ANALYSIS - Velocity error as a percentage of velocity computed as a function of velocity and path length.

to reduce velocity related errors when precise orientation of the instrument is possible. Note that all of these errors are reduced by increasing the spacing between the tines. However, the error surface suggests further reductions will be small once l is increased to 15 cm or 20 cm. Velocity resolution, as shown by Equation 13, is also improved with tine separation.

The resolution of turbulent eddies as they are advected through the measurement volume depends on both the path length, l, and the transducer diameter, d. The minumum sampling rate to avoid aliasing is $f_{s_{min}} = u/2l$ along the path and $f_{s_{min}} = u/2d$ across the path. The latter requirement is more stringent. For a 15 cm/s flow a 10 Hz minimum sampling rate is imposed by the transducer diameter. Note that these constraints apply to the resolution of turbulent eddies being advected through the beam that are smaller than the selected length scale. The first formula should not be interpreted as suggesting longer path lengths. First, the sampling rate is dictated by transducer diameter which is smaller than any reasonable tine spacing. Second, these formulas apply to the resolution of single eddies. Long acoustic paths necessarily average over multiple eddies of varying size degrading the resolution of the measurement. Resolving the smallest scales of flow requires short path lengths. Optimal path length, therefore, involves a balance between resolution and flow disturbance. A prototype with variable separation for testing is planned.

Vortex shedding occurs at the Strouhal frequency, $f_S = Su/D$, where S, the Strouhal number, is 0.2. The Strouhal signal in the spectrum will generally be outside of the wave band, but sampling at 10 Hz or more will be necessary to prevent aliasing for the expected range of wave orbital velocities.

Finally, Equation 13 shows that variations in sound speed can cause an error in the measurement. However,

a modification of the differential time circuit can measure the absolute sound speed, or the ambient temperature can be measured, and appropriate corrections can be applied.

V. ASSESSMENT

The primary advantage of the BASS Rake over the other techniques discussed in Section I is the ability to record spatially dense vertical profiles within a brief temporal window at a high rate. This is achieved with multiple measurement volumes and very high single measurement accuracy. Resolution of the first order dynamic structure of the wave bottom boundary layer is well within the instrument's capabilities.

Acoustic measurements are robust to the environment, having no great dependence on the presence of scatterers nor great sensitivity to fouling. Marine growth only presents a problem in the form of increased flow disturbance during long deployments. While some care must be taken with the tines, hot wires and films are far more fragile.

In cases where the viscous sublayer is a few millimeters or more thick it will be visible to the BASS Rake. Resolution of bursting and sweeping and of the smallest scales of turbulence is limited by the minimum spacing of the tines. This, in turn, is limited by the level of sensor induced flow disturbance that can be tolerated. The smaller sample volume of an LDV or hot wire would be an advantage here. Streaming in shallow shelf depths may be visible to this instrument, but will probably be obscured by turbulent fluctuations in deeper water. The BASS Rake is well suited for deployment on a flat or low relief bed and retains some utility among bedforms.

The Bass Rake is designed to make measurements in the continental shelf wave bottom boundary layer. It is also suitable for use in wave tanks and flumes where vertically detailed dynamic velocity profiles are commonly needed. In either setting it should not be viewed as a replacement for the other techniques discussed here. The BASS Rake is a complementary approach specifically designed to increase our knowledge of the dynamic structure of the continental shelf wave bottom boundary layer.

ACKNOWLEDGMENTS

I would like to express my thanks to Fred Thwaites, John Trowbridge, and Sandy Williams of WHOI for their many helpful suggestions during the writing of this paper.

REFERENCES

[1] Agrawal, Y. C., Aubrey, D. G., "Velocity Observations Above a Rippled Bed Using Laser-Doppler Velocimetry", *Journal of Geophysical Research* (1992), Vol. 97, pp. 20249-20260.

[2] Agrawal, Y. C., Trowbridge, J. H., Pottsmith, H. C., Oltman-Shay, J., "Velocity, Concentration, and Flux of Sediments in a Coastal Bottom Boundary Layer with a Laser Doppler Velocimeter", *Proceedings OCEANS '93*, IEEE/OES, October 1993, Vol. III, pp. 137-142.

[3] Batchelor, G. K., An Introduction to Fluid Dynamics, Cambridge University Press, Cambridge, 1967.

[4] Caldwell, D. R., Chriss, T. M., "The Viscous Sublayer at the Sea Floor", *Science* (1979), Vol. 205, No. 4411, pp. 1131-1132.

[5] Chriss, T. M., Caldwell, D. R., "Evidence for the Influence of Form Drag on Bottom Boundary Layer Flow", *Journal of Geophysical Research* (1982), Vol. 87, No. C6, pp. 4148-4154.

[6] Conley, D. C., Inman, D. L., "Field Observations of the Fluid-Granular Boundary Layer Under Near-Breaking Waves", *Journal of Geophysical Research* (1992), Vol. 97, No. C6, pp. 9631-9643.

[7] Grant, W. D., Madsen, O. S., "Combined Wave and Current Interaction With a Rough Bottom", *Journal of Geophysical Research* (1979), Vol. 84, No. C4, pp. 1797-1808.

[8] Grant, W. D., Madsen, O. S., "The Continental-Shelf Bottom Boundary Layer", *Annual Review of Fluid Mechanics* (1986), Vol. 18, pp. 265-305.

[9] Grant, W. D., Williams, A. J., 3rd, Glenn, S. M., "Bottom Stress Estimates and Their Prediction on the Northern California Continental Shelf During CODE 1: The Importance of Wave-Current Interaction", *Journal of Physical Oceanography* (1984), Vol. 14, pp. 506-527.

[10] Hart, D. D., Clark, B. D., "Fine-scale Field Measurement of Benthic Flow Environments Inhabited by Stream Invertibrates", *Bulletin of the North American Benthological Society* (1994), Vol. 11, pp. 174.

[11] Jonsson, I. G., Carlsen, N. A., "Experimental and Theoretical Investigations in an Oscillatory Turbulent Boundary Layer", *Journal of Hydraulic Research* (1976), Vol. 14, No. 1, pp. 45-60.

[12] Kundu, P. K., Fluid Mechanics, Academic Press, New York, 1990.

[13] Madsen, O. S., "Sediment Transport on the Shelf", Final Draft of Chapter III-6 of The Coastal Engineering Manual, to be published by the United States Army Corps of Engineers, Waterways Experiment Station, CERC, December 30, 1993.

[14] Morrison, A. T., III, Williams, A. J., 3rd, Martini, M., "Calibration of the BASS Acoustic Current Meter With Carrageenan Agar", *Proceedings OCEANS '93*, IEEE/OES, October 1993, Vol. III, pp. 143-148.

[15] Trivett, D. A., Terray, E. A., Williams, A. J., 3rd, "Error Analysis of an Acoustic Current Meter", *IEEE Journal of Oceanic Engineering* (1991), Vol. 16, No. 4, pp. 329-337.

[16] Trowbridge, J. H., Agrawal, Y. C., "Glimpses of a Wave Boundary Layer", submitted to the *Journal of Geophysical Research.*

[17] Wiberg, P. L., Harris, C. K., "Ripple Geometry in Wave-dominated Environments", *Journal of Geophysical Research* (1994), Vol. 99, No. C1, pp. 775-789.

[18] Williams, A. J., 3rd, Tochko, J. S., Koehler, R. L., Grant, W. D., Gross, T. F., Dunn, C. V. R., "Measurement of Turbulence in the Oceanic Bottom Boundary Layer with an Acoustic Current Meter Array", *Journal of Atmospheric and Oceanic Technology*, Vol. 4, No. 2, June 1987.